(2)

Dynamics of Separation and Reattachment in a Mach 5 Compression Ramp-Induced Shock Wave Turbulent Boundary Layer Interaction

Final Report

R. A. Gramann and D. S. Dolling

July 31, 1989

U. S. Army Research Office

Grant DAALO3-86-G-0045

The University of Texas at Austin
Aerospace Engineering and Engineering Mechanics Dept.

UNCLASSIFIED
SECURITY CLASSIFICATION OF THIS PAGE

REPORT DOCUMENTATION PAGE

1a. REPORT SECURITY CLASSIFICATION: Unclassified	1b. RESTRICTIVE MARKINGS
2a. SECURITY CLASSIFICATION AUTHORITY	3. DISTRIBUTION/AVAILABILITY OF REPORT: Approved for public release; distribution unlimited.
2b. DECLASSIFICATION/DOWNGRADING SCHEDULE	
4. PERFORMING ORGANIZATION REPORT NUMBER(S)	5. MONITORING ORGANIZATION REPORT NUMBER(S): ARO 23763.3-EG-F
6a. NAME OF PERFORMING ORGANIZATION: University of Texas at Austin; 6b. OFFICE SYMBOL (If applicable):	7a. NAME OF MONITORING ORGANIZATION: U. S. Army Research Office
6c. ADDRESS (City, State, and ZIP Code): Aerospace Engineering Department WRW 217, Austin, TX 78712	7b. ADDRESS (City, State, and ZIP Code): P. O. Box 12211 Research Triangle Park, NC 27709-2211
8a. NAME OF FUNDING/SPONSORING ORGANIZATION: U. S. Army Research Office; 8b. OFFICE SYMBOL (If applicable):	9. PROCUREMENT INSTRUMENT IDENTIFICATION NUMBER: DAAL03-86-G-0045
8c. ADDRESS (City, State, and ZIP Code): P. O. Box 12211 Research Triangle Park, NC 27709-2211	10. SOURCE OF FUNDING NUMBERS: PROGRAM ELEMENT NO. / PROJECT NO. / TASK NO. / WORK UNIT ACCESSION NO.

11. TITLE (Include Security Classification)
DYNAMICS OF SEPARATION AND REATTACHMENT IN A MACH 5 COMPRESSION RAMP FLOW.

12. PERSONAL AUTHOR(S)
R. Gramann, D. S. Dolling

13a. TYPE OF REPORT	13b. TIME COVERED	14. DATE OF REPORT (Year, Month, Day)	15. PAGE COUNT
Final	FROM 6/1/86 TO 5/31/89	August 7, 1989	35

16. SUPPLEMENTARY NOTATION
The view, opinions and/or findings contained in this report are those of the author(s) and should not be construed as an official Department of the Army position, policy, or decision, unless so designated by other documentation.

17. COSATI CODES			18. SUBJECT TERMS (Continue on reverse if necessary and identify by block number)
FIELD	GROUP	SUB-GROUP	Shock Wave Turbulent Boundary Layer Interaction
			Unsteady Flow
			Turbulent Separation

19. ABSTRACT (Continue on reverse if necessary and identify by block number)

The separation process in cylinder and unswept compression ramp induced shock wave turbulent boundary layer interactions has been examined using a conditional-analysis of wall pressure fluctuation measurements. The tests were performed in a Mach 5 blowdown tunnel under adiabatic wall temperature conditions. The conditional analysis has shown that the instantaneous separation position is at or close to the instantaneous separation shock foot in these interactions. The separation line as indicated by traditional surface tracer methods is at, or close to, the downstream boundary of a region of intermittent separation. The dynamics of the separation bubble in the unswept compression ramp flowfield have also been examined and initial results suggest that the motion of the separation point and reattachment point locations are correlated. The preliminary results indicate the reattachment point is at its downstream locations when the separation shock is at its upstream locations.

20. DISTRIBUTION/AVAILABILITY OF ABSTRACT ☐ UNCLASSIFIED/UNLIMITED ☐ SAME AS RPT. ☐ DTIC USERS	21. ABSTRACT SECURITY CLASSIFICATION: Unclassified
22a. NAME OF RESPONSIBLE INDIVIDUAL	22b. TELEPHONE (Include Area Code) / 22c. OFFICE SYMBOL

DD FORM 1473, 84 MAR — 83 APR edition may be used until exhausted. All other editions are obsolete.

SECURITY CLASSIFICATION OF THIS PAGE
UNCLASSIFIED

TABLE OF CONTENTS

LIST OF FIGURES

LIST OF TABLES

LIST OF APPENDICES

Statement of Problem

The purpose of this study was to investigate the dynamics of the separation bubble in an unswept compression ramp-induced shock wave turbulent boundary layer interaction. This flowfield has been examined numerous times in earlier studies, with a variety of techniques[1-7]. These studies have addressed several features of this flowfield, such as spanwise variations (three dimensional structures/effects), the separation shock motion, and mean features of the flowfield, including the overall structure. However, little time dependent information on the separation process, the separation bubble, or the region of reattachment has been obtained. To develop a complete understanding of the interaction, information on these latter aspects of the flow must be known. In particular, information on the separation bubble is needed to complete the overall flowfield picture. With a complete time-dependent description of the interaction, insight into the physical mechanisms controlling this interaction will be available. This insight will also provide guidance for the required improvement in the numerical models being used to predict these interactions.

Summary of Results

To date, several interesting results have been obtained through the test and analysis program performed under this grant. Some of these have already been published and consequently will only be summarized here. Continuing work, needed for answering one or two remaining questions will also be described.

First, a method of determining flow direction using wall pressure fluctuations has been developed and has been used to detect separated flow in two interactive flowfields. Two channels of wall pressure fluctuations from two closely spaced high frequency pressure transducers are used in the method. Thus the method is non-intrusive and relatively easy to use. Kulite miniature pressure transducers are mounted flush with the test surface, in the region of the interaction of interest. Figure 1 shows a centerline view of one interaction and one typical instrumentation arrangement. In this figure, the transducers are located in the intermittent region, which is characterized by large pressure fluctuations due to the separation shock oscillations within this region. The percentage time that a position in the intermittent region is downstream of the separation shock is known as that location's "intermittency" (γ) value. The upstream boundary of the intermittent region is

the upstream boundary of the interaction (γ=0%). The downstream boundary of the intermittent region (γ=100%) is typically delineated by the separation line determined using surface tracers. Downstream of this point, the flow is fully separated at all times.

Continuous data, sampled simultaneously on the two channels at rates ranging from 200 to 500 kHz are stored in CPU memory and then transferred to disk. Analysis is then performed on the data. By cross correlating selected data corresponding to a certain flow conditions, features of that flow, such as flow direction and time-averaged large scale structure velocity, can be determined. This analysis method, described in detail in Publication 2(see p. 24), was used to determine the features of the separated region in the 28° compression ramp induced interaction. The freestream Mach number was 4.95. Wall conditions were nearly adiabatic; the boundary layer on the tunnel floor developed naturally and was fully turbulent at the test locations. Additional flow conditions are given in Table 1.

Separation process:

The analysis method described briefly above has been used to examine the separation process in a shock wave turbulent boundary layer interaction. Data from a cylinder induced interaction and a compression ramp interaction

have been analyzed and several interesting points concerning separation have been clarified. Figure 2 shows cross correlation results obtained using the signals from two pressure transducers placed just downstream of 'S,' the separation line determined using surface tracers. The transducers were mounted in the streamwise direction, spaced 0.292 cm apart. Both the cylinder and ramp cross correlations show a distinctive double peak, indicative of separated flow. A more detailed discussion of this result is presented in Appendix A.

To determine flow direction in the intermittent region, data corresponding to flow downstream of the separation shock were extracted from continuous time data obtained with both transducers mounted in the intermittent region. Upstream of the separation shock, undisturbed boundary layer flow exists. Hence the direction and broadband velocities for this portion of the flow are known. The "Conditionally Extracted Analysis Data Sets" (CEADS) corresponding to flow downstream of the separation shock were analyzed using the cross correlation algorithm. Using the cross correlations, the flow direction and velocities downstream of the shock can be calculated. Figure 3 shows several results from locations in the intermittent region of a cylinder induced interaction. The "double peak" pattern, indicative of separated flow, is clear and has the same timing as those in Figure 2. Thus separation occurs

immediately downstream of the separation shock at all locations within the intermittent region of the cylinder induced interaction.

Similar analyses of ramp induced interaction data were performed as well. Typical results are shown in Fig 4. Again, separated flow characteristics are seen in the cross correlation at several locations within the intermittent region. Thus separation occurs within the intermittent region, immediately downstream of the oscillating separation shock. Both cylinder and unswept compression ramp induced interactions exhibit this feature. Therefore, the intermittent region is a region of intermittent separation. Further, the separation line,'S,' is close to the downstream boundary of this region of intermittent separation. A physical explanation of this phenomenon is provided in Appendix B.

Separation Bubble Dynamics:

Data have been obtained in the separated flow (i.e. downstream of 'S') of the unswept compression ramp induced interaction, both upstream of the ramp corner and on the ramp face. The data just upstream of the ramp corner have been used to characterize the separated flow on the ramp face. Figure 5 shows a cross correlation result obtained with both transducers closer to the ramp, along with the previous result shown in Fig. 2. This result is

characteristic of separated flow near the ramp corner and will be used for comparison with cross correlations on the ramp face.

Data near reattachment have been obtained for two separation shock positions, as well as continuous time. 800 records total are obtained during the continuous time data acquisition, providing approximately one second of continuous time data. These data have been analyzed to determine if information regarding the the separated flow can be obtained near reattachment. Based on data obtained for fixed separation shock position, the preliminary results indicate that reattachment (or the flow character near reattachment) is dependent on the shock position. Figures 6 and 7 show the mean pressure and RMS of the wall pressure fluctuations distributions within the interaction. The time-averaged results are similar to results obtained by other investigators in other facilities[1-5]. It is interesting to note that the mean pressure and RMS for the furthest upstream separation shock location (γ = 0-8%) are significantly less than the continuous time values. When the separation shock is between γ = 30% and γ = 40%, the mean pressure and RMS are approximately equal to the continuous time pressures. This suggests that the wall pressure and its fluctuations on the ramp face are a function of separation shock position. Further data are currently being obtained to expand the regions measured on the ramp face and increase the number of

shock positions examined.

Cross correlations were calculated from data from three pairs of transducers located near 'R,' the reattachment line determined using surface tracers. Results at one mid-ramp location, appoximately 1.6 δ_o downstream of 'R,' were also obtained. Figures 8-11 show the resulting cross correlations of the wall pressure fluctuations for each position. In each figure, both continuous time data and specific shock position data (or "shock-fixed") data are presented.

Figure 8 shows the results with both transducers located upstream of the reattachment line, 'R.' Although a change in magnitude in the correlation coefficients is seen, the character of the cross correlations from the three data sets are the same. Figure 9 shows cross correlations of data from two transducers straddling 'R.' A change in character is seen between the continuous data result and the "shock-fixed" results. Specifically, the distinct dips on either side of the dominant peak are present in the "shock-fixed" data, but are barely perceptable at $-\tau$ for continuous time data. Figure 10 shows the same trend. The dips are less pronounced for the "shock-fixed" data, and no dip is seen in the continuous time result. Both transducers in this case are mounted close to, but downstream of 'R.' The "dips" are indicative of

separated flow. Further downstream on the ramp face, separated flow exists for a smaller fraction of the time. Thus the continuous time signals show less and less of the separated characteristics (i.e. cross correlation "dips") as distance downstream of the ramp corner is increased. However, the shock-fixed data clearly show the separated character exists at positions downstream of 'R.' At these locations, little indication of separated flow in the continuous data cross correlation exists.

Figure 11 shows the correlations of signals from transducers mounted at mid-ramp locations. No change in the cross correlations for the 3 cases (i.e. continuous time, γ = 0-8%, and γ = 30-40%) is seen. This confirms the sensitivity of the method for the locations closer to the ramp corner. These data suggest the reattachment point motion is correlated with the separation shock motion. If no correlation with shock position existed, the shock-fixed data would repeat the continuous time data, since random data sets (i.e. data sets corresponding to different flow conditions) would be used to used to calculate the shock-fixed cross correlations. The continuous time data has all flow conditions for a given position represented in its results. Since a change occurs when shock-fixed data is used only certain flow conditions are occuring for a given separation shock location. Additional data are needed to expand the information available, both for more shock positions and ramp

locations. These data necessary to verify these conclusions are currently being acquired.

Thus, preliminary results suggest the flow character at locations near reattachment are dependent on separation shock position (or separation point position). The results suggest that when the separation shock is upstream, the reattachment point is downstream.

The shock motion/reattachment point motion result is further substantiated by turning angle calculations in the intermittent region based on the pressure rise across the separation shock. The pressure rise turning angles indicate, using a straight line approximation for the separation bubble boundary, that the reattachment point moves approximately 0.1 inch with separation shock motion ranging from $\gamma = 0\%$ to $\gamma = 100\%$. The reattachment point is at its upstream location when the shock is downstream (high γ), and vice versa. Figure 12 shows a sketch of the approximated flowfield.

Summary:

The separation process in cylinder and unswept compression ramp induced shock wave turbulent boundary layer interactions has been examined. Separation occurs across the separation shock in these interactions. Thus the

intermittent region is also a region of intermittent separation. The separation line determined using surface tracer methods is at, or very close to, the downstream boundary of this intermittent separation region.

The separation bubble in an unswept compression ramp flowfield has been examined and initial results suggest the separation point and reattachment point locations are correlated. Cross correlations near reattachment are dependent on separation shock position. The preliminary results indicate the reattachment point is at its downstream locations when the separation shock is at its upstream locations. Further information on the downstream shock locations will be obtained shortly, completing the data base.

The time dependent pressure values in the intermittent region and on the ramp face are substantially different from the time-averaged values. This suggests that the computational models being used to calculate these flowfields must incorporate these time dependent phenomena before adequate results will be obtained. The mean results are not an sufficiently accurate representation of the flowfield.

Wind Tunnel Flow Conditions	
Parameter	Tunnel Floor
M_∞	$4.90 \pm .02$
U_∞	741 m/s (2432 ft/s)
Re_∞	53.3×10^6 m^{-1} (16.2×10^6 ft^{-1})
T_o	330°K (595°R)
P_o	2.09×10^6 N/m^2 (304 psi)
X	0.74 m (29 in) from throat
δ_o	1.62×10^{-2} m (0.63 in)
δ^*	5.23×10^{-3} m (0.206 in)
θ	4.54×10^{-4} m (1.83×10^{-2} in)
Π	0.115
Re_θ	23.4×10^3
C_f	9.9×10^{-4}

Table 1 Freestream and Boundary Layer Conditions

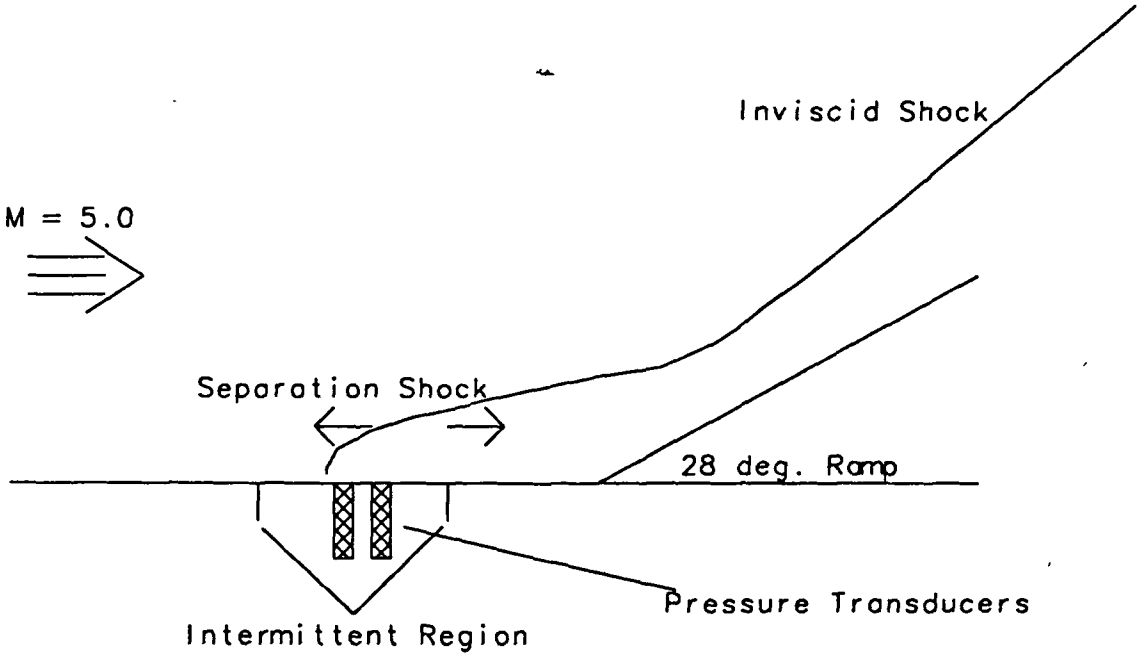

Figure 1 - Sideview of Flowfield with Instrumentation Installed

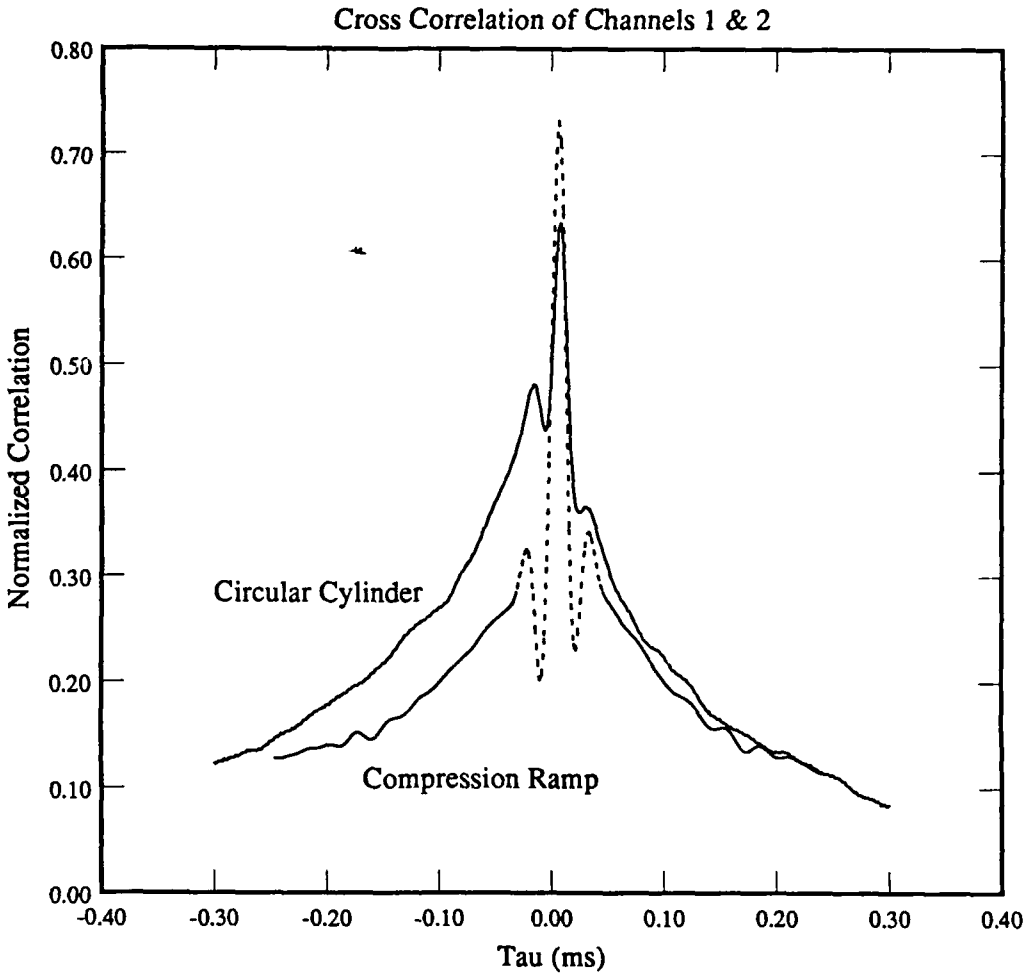

No. of anal records/channel - 400
No. of data records/channel - 400
Sampling frequency - 500000.0

Figure 2 - Separated Cross Correlations

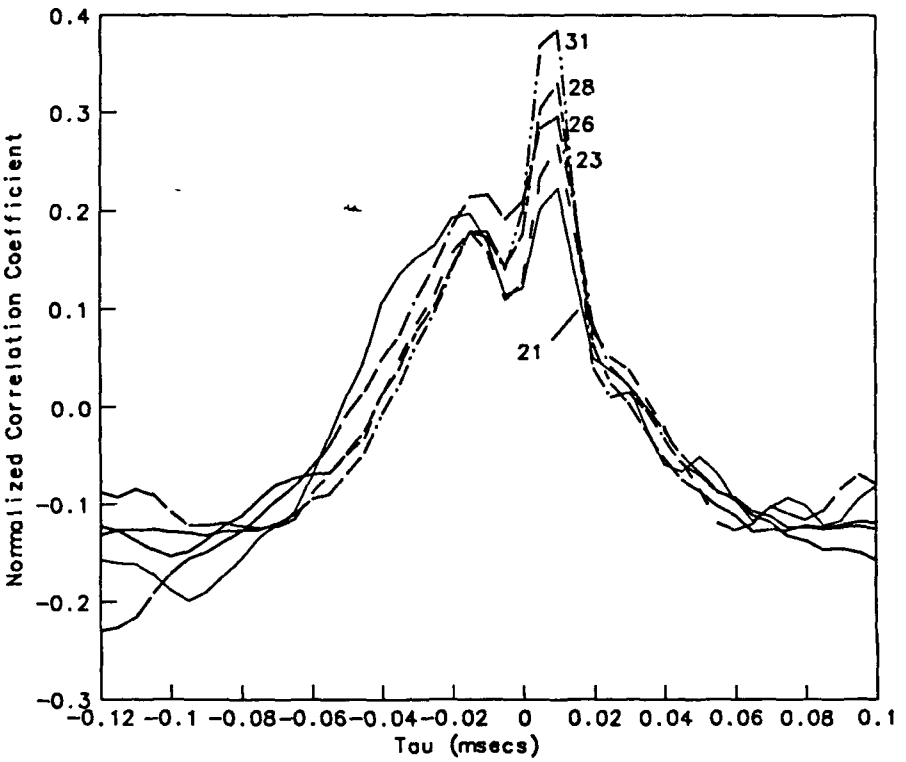

Run	$(X/D)_1$	$(X/D)_2$	$Gamma_1$	No. of CEADS
21	2.89	2.73	8.47	133
23	2.83	2.68	15.9	222
26	2.63	2.47	32.4	1457
28	2.57	2.42	37.73	1229
31	2.37	2.21	75.5	3018

Figure 3 - Conditional Cross Correlations, Circular Cylinder

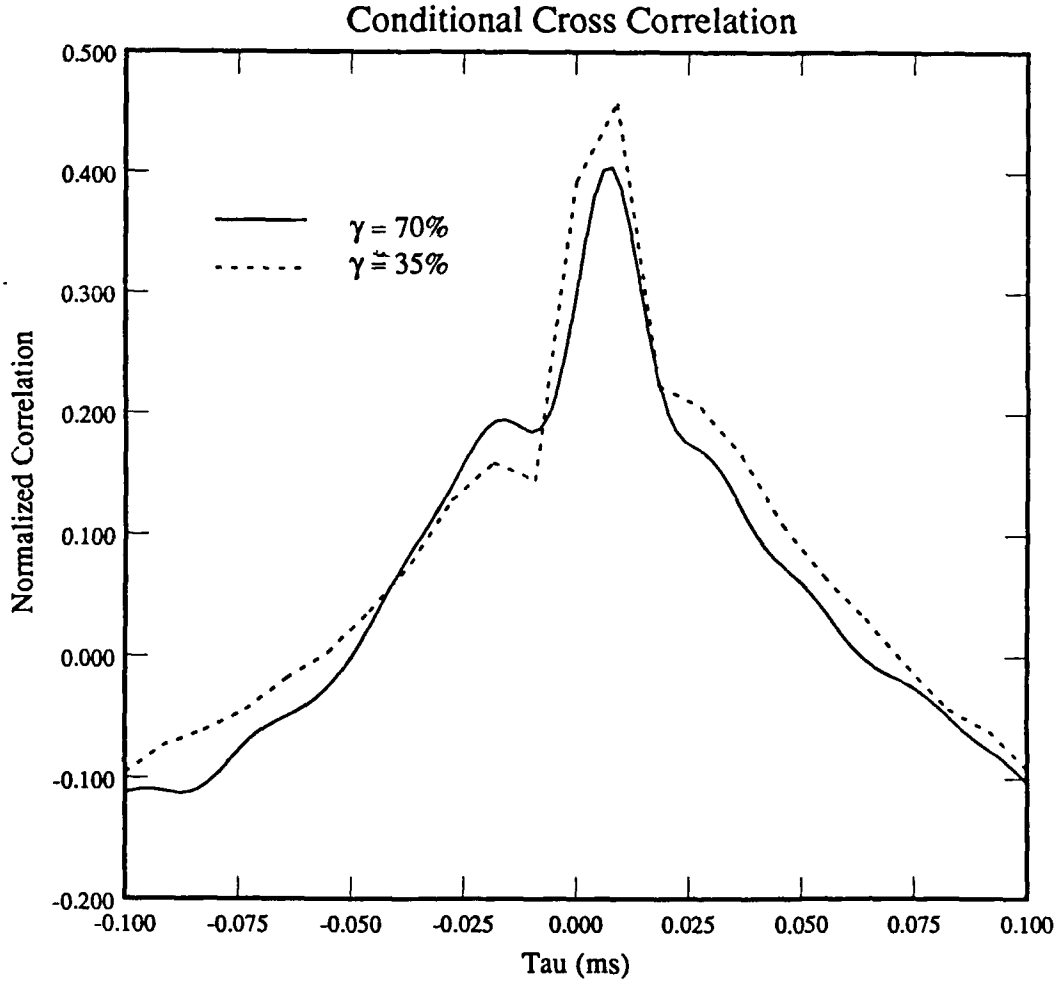

Upper Threshold - 0.900
Lower Threshold - 0.75
Size of CEADS - 128 and 32
No. of data records- 400 and 100
Sampling frequency - 500 and 109 kHz

Figure 4 - Conditional Cross Correlation, Compression Ramp

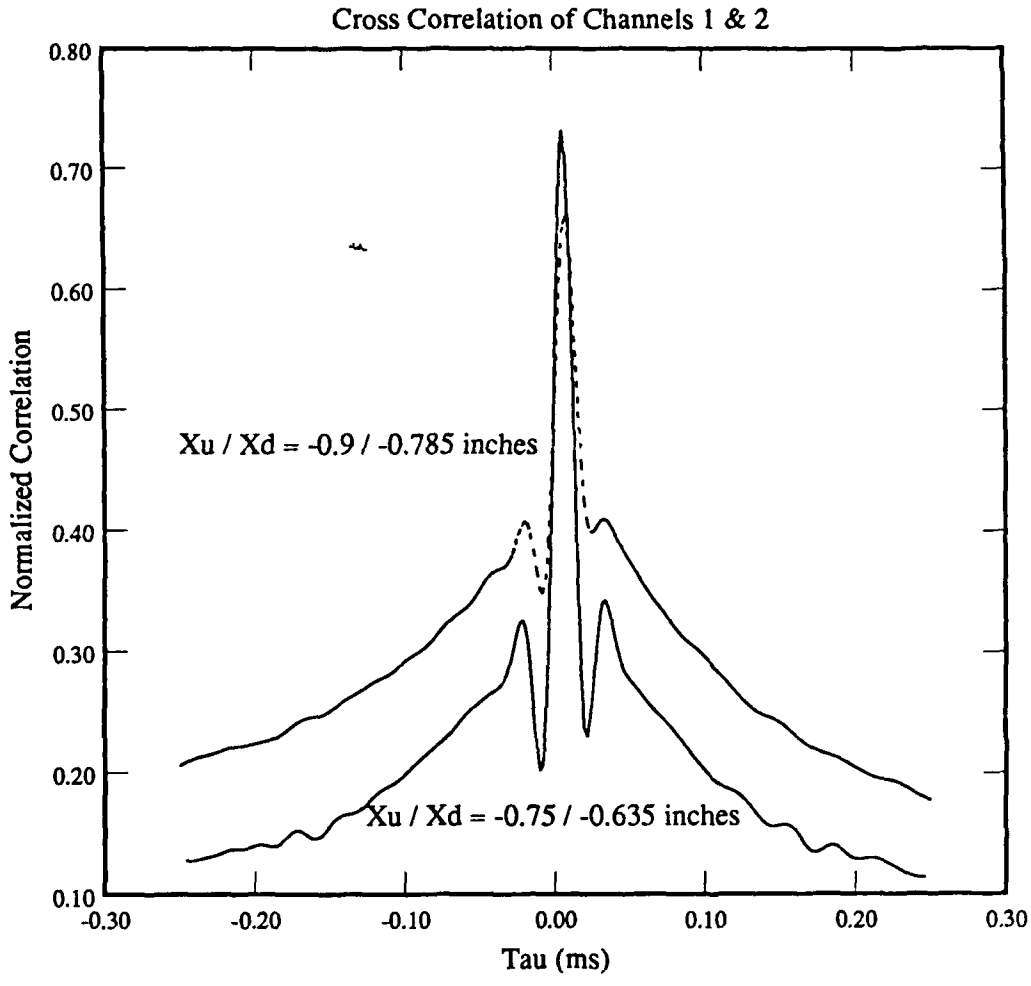

No. of anal records/channel - 400
No. of data records/channel - 400
Sampling frequency - 500000.0

Figure 5 - Separated Cross Correlations-Compression Ramp

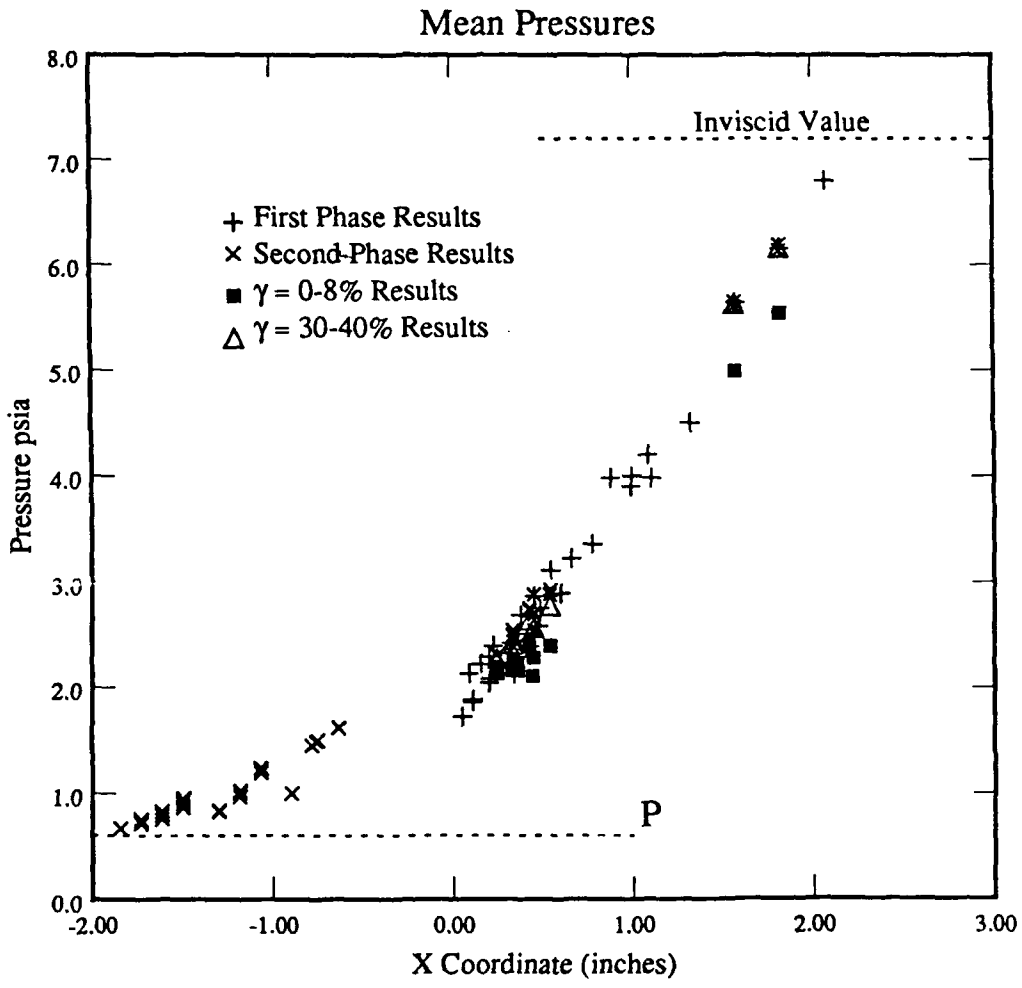

Figure 6 - Time-Averaged Pressure Distribution

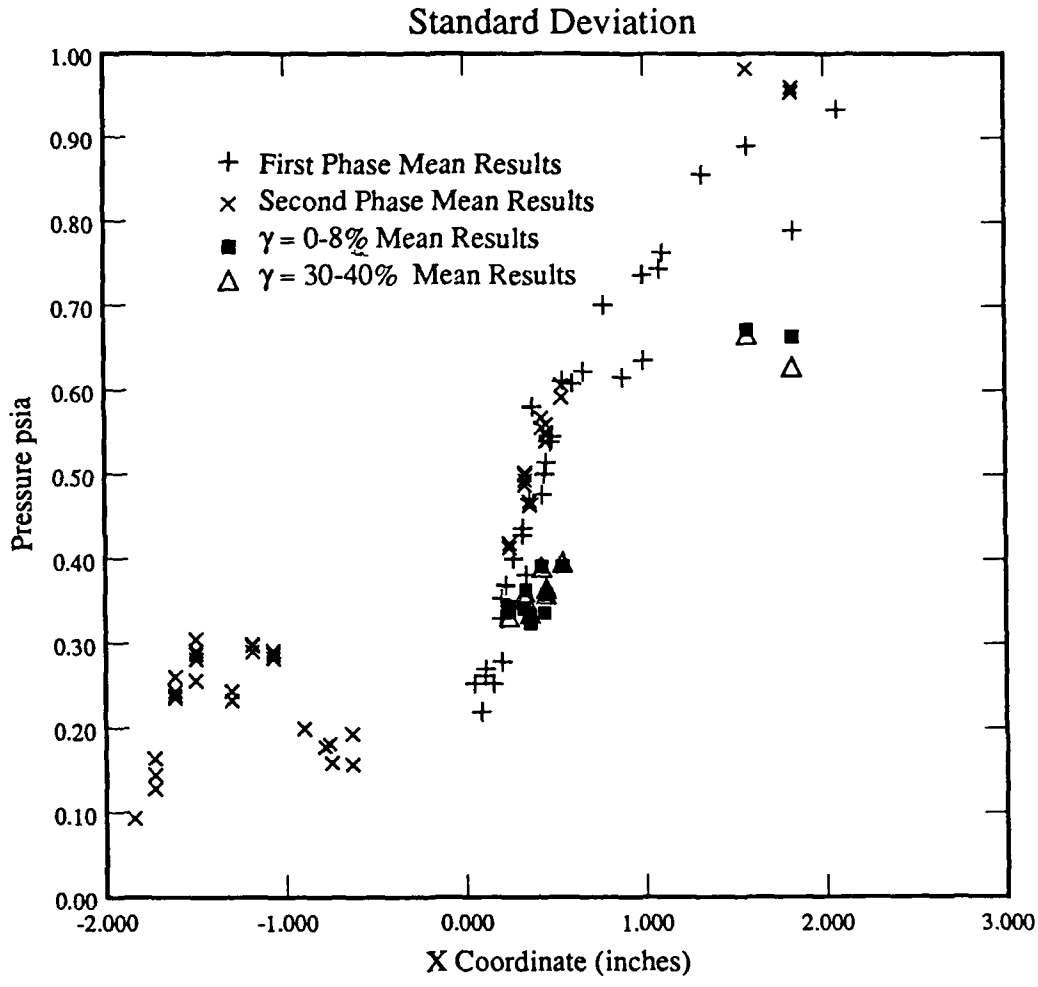

Figure 7 - Wall Pressure RMS Distribution

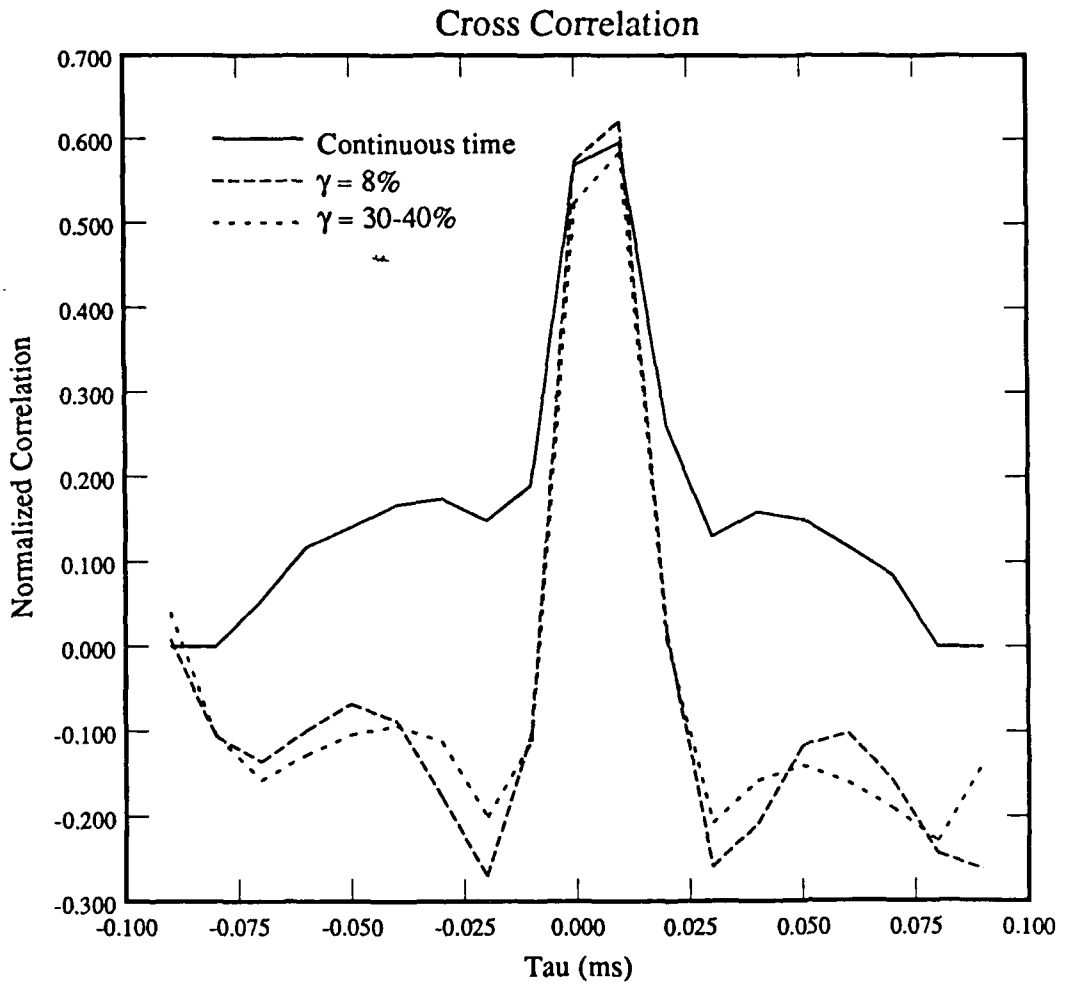

Analysis of Reattachment Locations
Upstream Ramp Transducer at X = 0.245 inches (#3)
Downstream Ramp Transducer at X = 0.36 inches (#4)
Sampling frequency - 100000.0

Figure 8 - Cross Correlations Upstream of 'R'

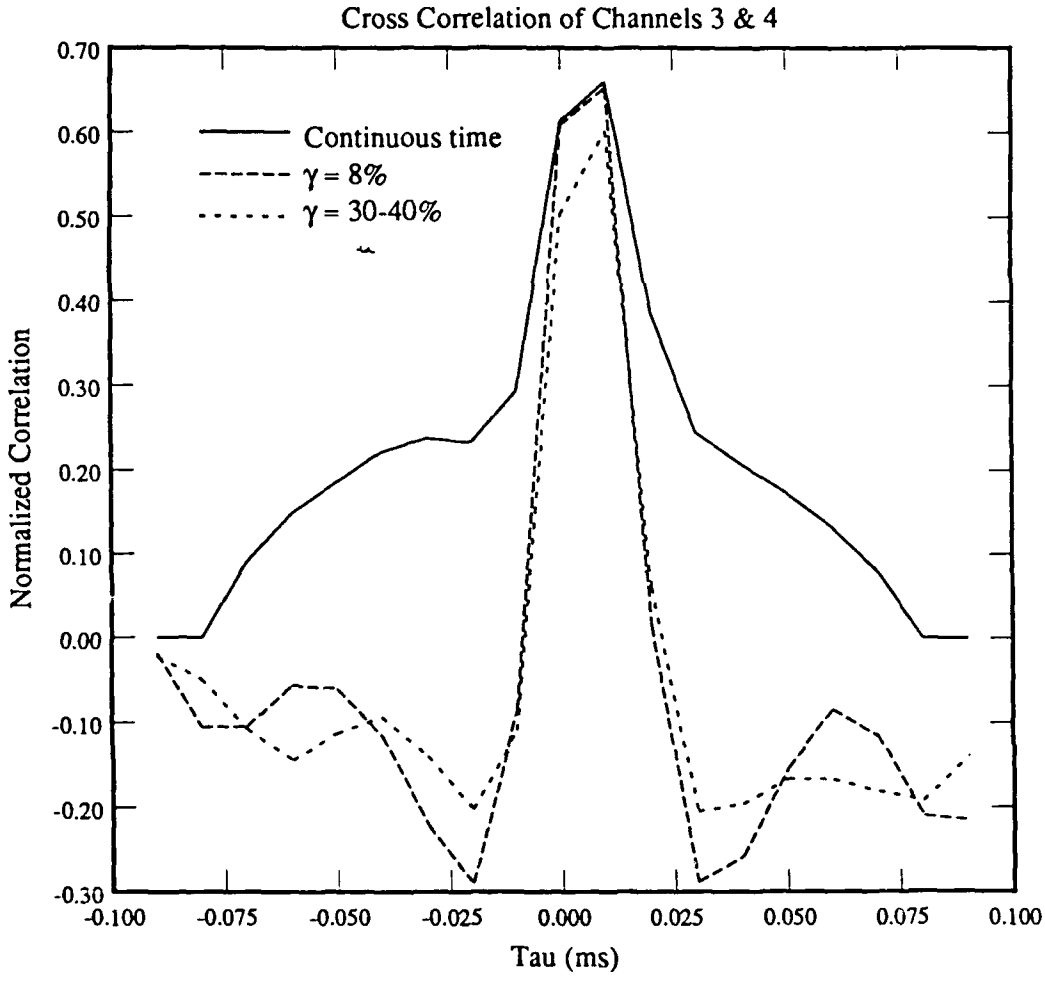

Analysis of Reattachment Locations
Upstream Ramp Transducer at X = 0.335 inches (#3)
Downstream Ramp Transducer at X = 0.45 inches (#4)
Sampling frequency - 100000.0

Figure 9 - Cross Correlations Near 'R'

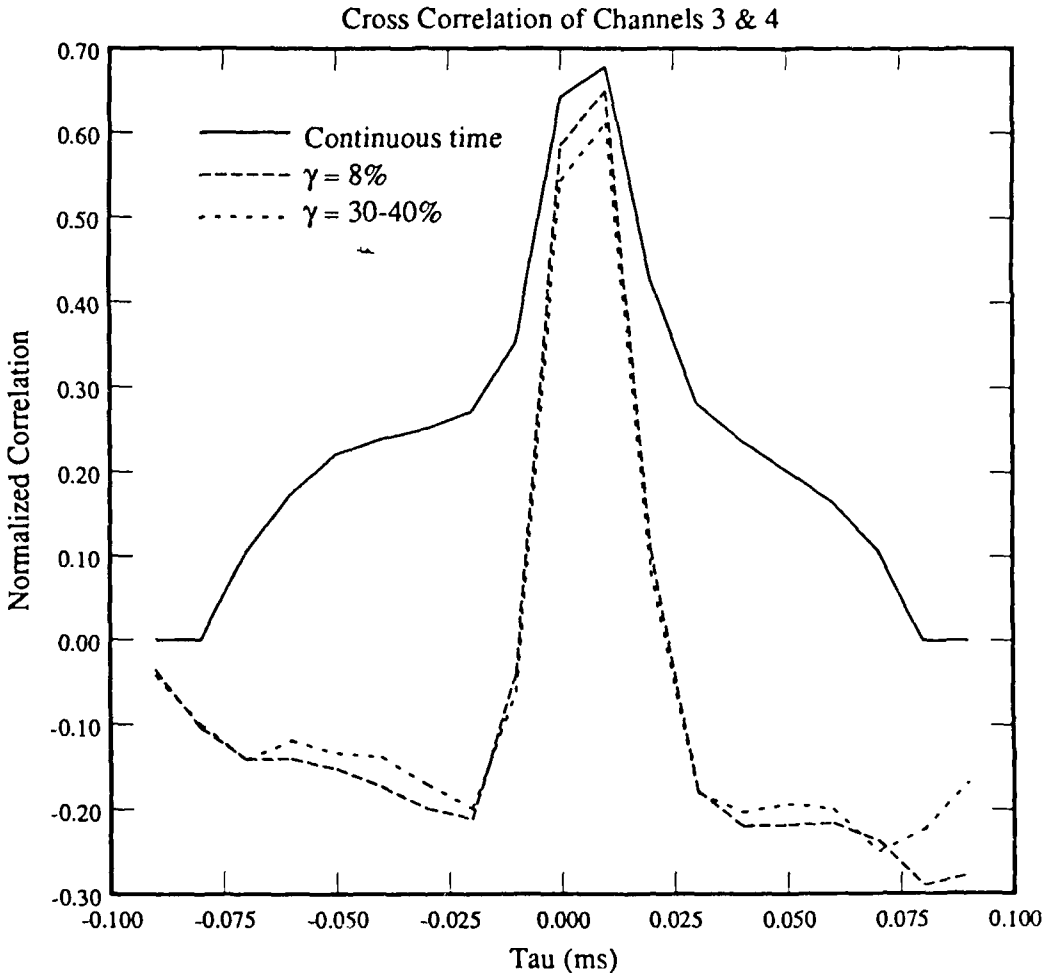

Analysis of Reattachment Locations

Upstream Ramp Transducer at X = 0.425 inches (#3)
Downstream Ramp Transducer at X = 0.54 inches (#4)
Sampling frequency - 100000.0

Figure 10 - Cross Correlations Downstream of 'R'

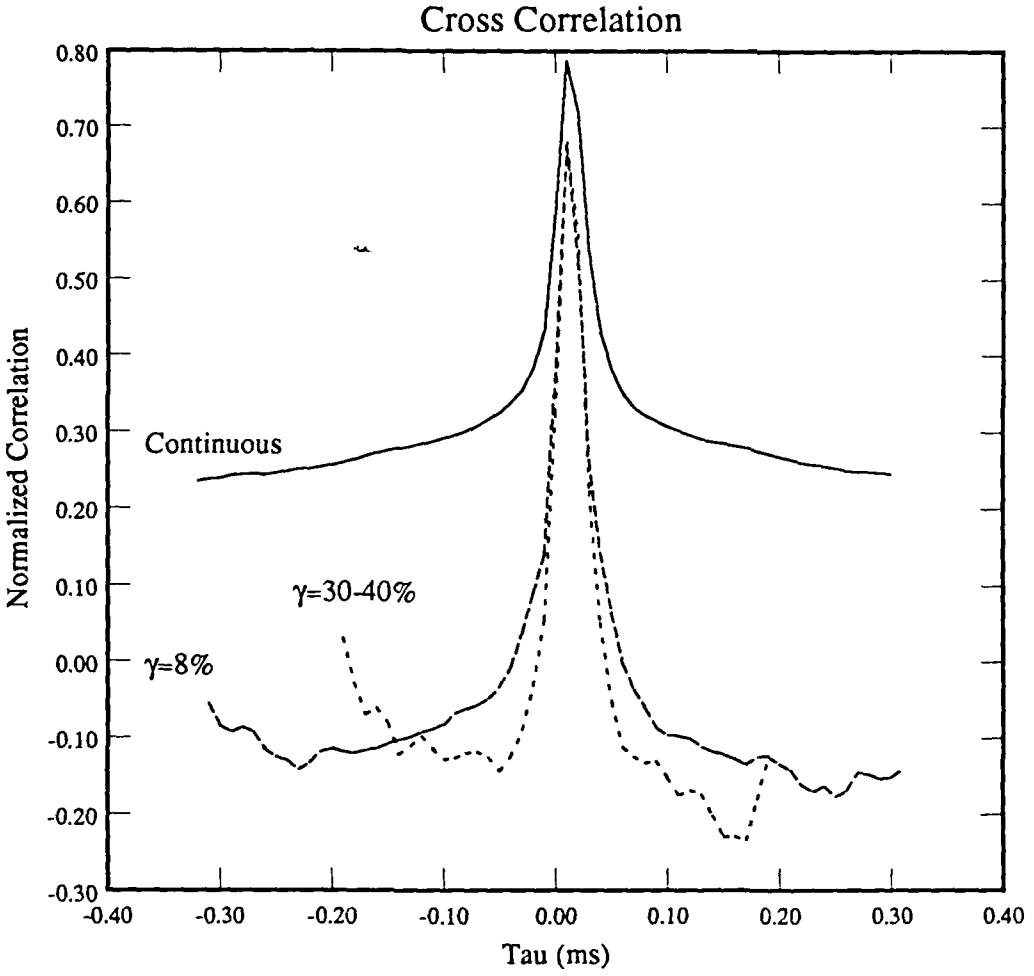

Upstream Ramp Transducer at X = 1.57 inches (#11)
Downstream Ramp Transducer at X = 1.82 inches (#12)
Sampling frequency - 100000.0

Figure 11 - Cross Correlations at Mid-Ramp Location

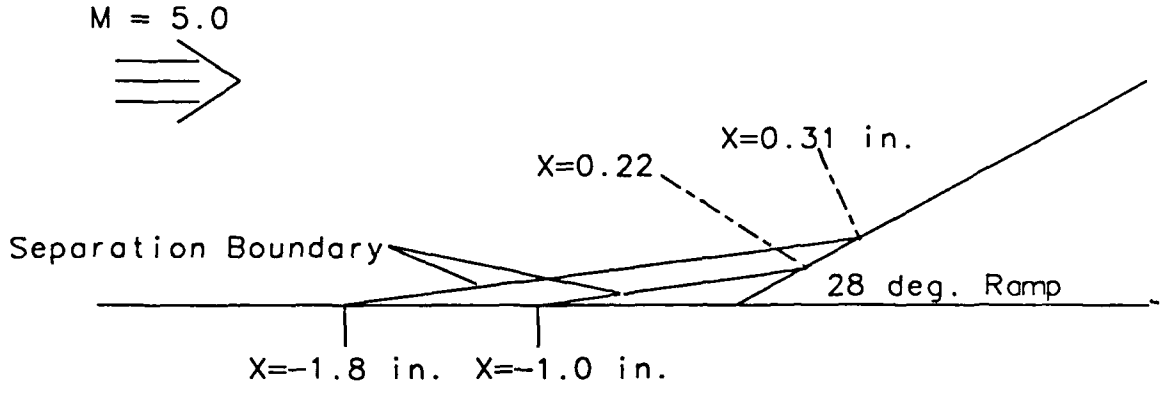

Figure 12 - Simplified Flowfield

LIST OF PUBLICATIONS

1 Gramann, R. A. and D. S. Dolling, "Interpretation of Separation Lines in Shock Induced Turbulent Flows," *AIAA Journal,* Vol. 25, No. 12, December 1987, pp. 1545-1546.

2 Gramann, R. A. and D. S. Dolling, "Detection of Shock Induced Separation Using Wall Pressure Fluctuations," AIAA Paper 88-4676, AIAA Measurements and Instrumentation Conference, Atlanta, GA, September 1988.

LIST OF PARTICIPATING PERSONNEL

R. A. Gramann, Graduate Research Assistant,

anticipated Ph.D. graduation date: December 1989.

REFERENCES

[1] Andreopoulos, J. and K.C. Muck, "Some New Aspects of the Shock Wave Boundary Layer Interaction in Compression Ramp Flows," AIAA Paper 86-0342.

[2] Dolling, D.S. and M. T. Murphy, "Unsteadiness of the Separation Shock Wave in a Supersonic Compression Ramp Flowfield," *AIAA Journal*, Vol 21, No. 12, pp.1628-1634.

[3] Dolling, D.S. and C. T. Or, "Unsteadiness of the Shock Wave Structure ins Attached and Separated Compression Corner Flowfields," AIAA Paper 83-1715.

[4] Selig, M.S., J. Andreopoulos, K.C. Muck, J.P. Dussuage, and A.J. Smits, "Simultaneous Wall-Pressure and Mass-Flux Measurements Downstream of a Shock Wave Turbulent Boundary Layer Interaction," AIAA Paper 87-0550.

[5] Muck K.C., J.P. Dussuage, and S.M. Bogdonoff, "Structure of the Wall Pressure Fluctuations in a Shock Induced Separated Turbulent Flow," AIAA Paper 85-0179.

[6] Settles, G.S., "An Experimental Study of Compressible Turbulent Boundary Layer Separation at High Reynolds Numbers," Ph. D. Thesis, Princeton University, 1975.

[7] Nordyke, R.J., "Spanwise Properties of the Unsteady Separation Shock in a Mach 5 Unswept Compression Ramp Interaction," M.S. Thesis, Dept. Aerospace Engineering and Engineering Mechanics, The University of Texas at Austin, December 1987.

Appendix A

AIAA'88

AIAA-88-4676

Detection of Turbulent Boundary Layer Separation Using Fluctuating Wall Pressure Signals

R. A. Gramann and D. S. Dolling,
Dept. of Aerospace Engineering and Engineering Mechanics, The University of Texas at Austin

AIAA/NASA/AFWAL Conference on Sensors and Measurements Techniques for Aeronautical Applications

September 7-9, 1988/Atlanta, Georgia

Detection of Turbulent Boundary Layer Separation Using Fluctuating Wall Pressure Signals

R. A. Gramann[+] and D. S. Dolling[*]
Dept. of Aerospace Engineering and Engineering Mechanics
The University of Texas at Austin

Abstract

A technique for detecting intermittent shock-induced turbulent boundary layer separation has been developed and tested in a Mach 5 blowdown tunnel. The interaction was generated by "semi-infinite" circular cylinders. The method employs two miniature pressure transducers oriented streamwise and installed flush with the test surface. Through cross correlations of the conditionally sampled signals of the two transducers under the moving shock it has been shown that the flow downstream of the instantaneous shock position is separated. The results indicate that in these flows, the separation location indicated by surface tracers, such as the kerosene lampblack method, is actually the downstream boundary of a region of intermittent separation.

Introduction

Surface tracer techniques, such as the kerosene lampblack method, are widely used in high speed flows to find "separation lines" or "lines of coalescence," particularly in shock wave turbulent boundary layer interactions[1]. These methods are relatively easy to use and produce highly defined, repeatable "separation lines". In the case of the kerosene-lampblack method, in which the pattern is lifted off the surface on large sheets of transparant tape, full scale undistorted records are obtained. Measurements of angles and length scales are easily made from these patterns and are widely used for comparison with numerical simulation results.

In many shock wave boundary layer interactions, wall pressure fluctuation measurements have shown that the separation shock is unsteady, generating an intermittent wall pressure signal[2-7]. A typical example, in a Mach 3 blunt fin interaction, is shown in Figure 1. This region of shock motion is known as the intermittent region. Intermittency, γ, is defined as the fraction of time a pressure transducer is downstream of the shock, and is an indication of location within the intermittent region. The intermittent region extends from where the incoming flow is first disturbed by the shock, to close to the separation line, 'S', indicated by surface tracers.

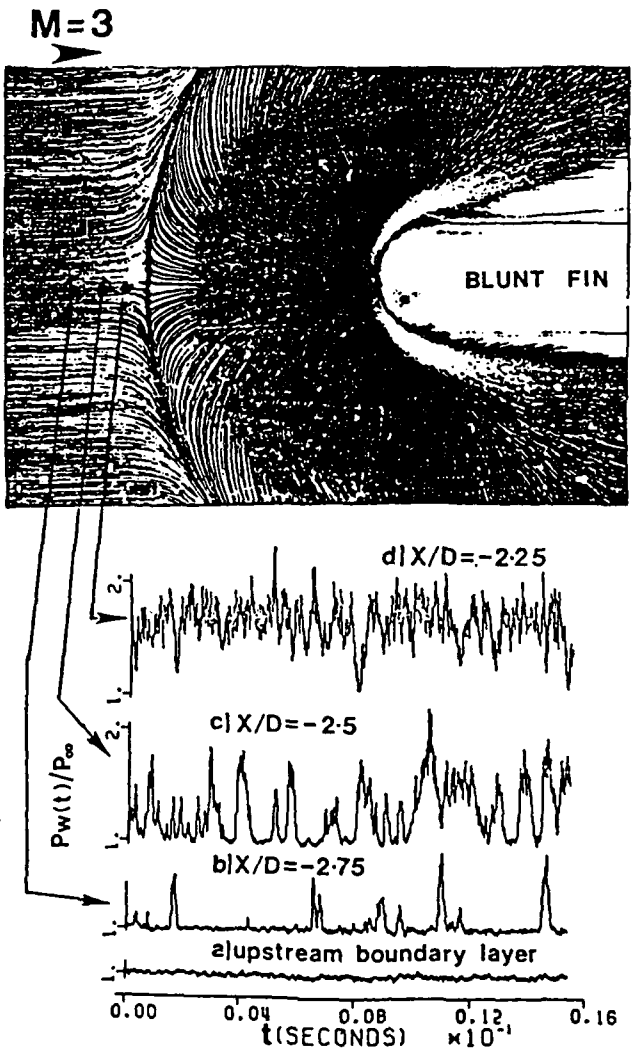

Figure 1 Kerosene Lampblack Flow Visualization and Wall Pressure Fluctuations

[+] Graduate Research Assistant, Member AIAA
[*] Associate Professor, Associate Fellow AIAA

In such flows where the separation shock is highly unsteady, the physical meaning of these surface tracer lines has recently come into question. In particular, does backflow actually occur upstream of the surface tracer line? This might occur since the surface tracer material responds to the mean wall shear stress, and the technique has essentially zero frequency response. Further, the mean wall shear stress at a point is the result of two flow fields which are present in the intermittent region (i.e. the undisturbed flow upstream of the shock, and the "disturbed" flow downstream of the shock). What is needed to understand what the surface tracer lines in this region actually represent are instantaneous flow direction measurements close to the surface. Unlike incompressible flow, where instantaneous flow direction measurement techniques, such as thermal tufts, are reasonably well developed[8,9], no relatively straightforward, measurement techniques have been developed for high speed flows. Therefore, the need for a relatively simple method of detecting "instantaneous" flow direction is clearly evident.

The objective of the work reported in this paper was to determine if flow direction could be deduced from wall pressure fluctuations. A method of doing this, using high frequency response pressure transducers, and standard signal conditioning instrumentation has been developed and tested in a Mach 5 shock wave turbulent boundary layer interaction. Although considerable care is needed in transducer installation, calibration and use, such measurements are non-intrusive, and can be made relatively easily and routinely in high speed flows. The equipment, technique, analysis involved, and some results are presented in this paper.

Experimental Program

Wind Tunnel and Test Conditions

All data were obtained on the tunnel floor of the University of Texas Blowdown Wind Tunnel under essentially adiabatic wall temperature conditions. The facility has a 17 x 15 cm test section and operates at a nominal freestream Mach number of 4.9. The boundary layer developed naturally and was fully turbulent at the test location. Table 1 gives the incoming boundary layer and freestream properties as deduced from pitot surveys. The models used for the study were circular cylinders, 1.27 and 1.9 cm in diameter, 8.9 cm and 7.6 cm high respectively. Based on the criterion of Ref. 10, both cylinders were effectively semi-infinite. The position of the cylinders could be varied relative to the fixed location of the instrumentation plug described below so that different regions of the flow field could be examined (Fig. 2).

Wind Tunnel Flow Conditions	
Parameter	Tunnel Floor
M_∞	4.90 ± .02
U_∞	741 m/s (2432 ft/s)
Re_∞	53.3×10^6 m^{-1} (16.2×10^6 ft^{-1})
T_0	330°K (595°R)
P_0	2.09×10^6 N/m^2 (304 psi)
X	0.74 m (29 in) from throat
δ_0	1.62×10^{-2} m (0.63 in)
δ^*	5.23×10^{-3} m (0.206 in)
θ	4.54×10^{-4} m (1.83×10^{-2} in)
Π	0.115
Re_θ	23.4×10^3
C_f	9.9×10^{-4}

Table 1 Freestream and Boundary Layer Conditions

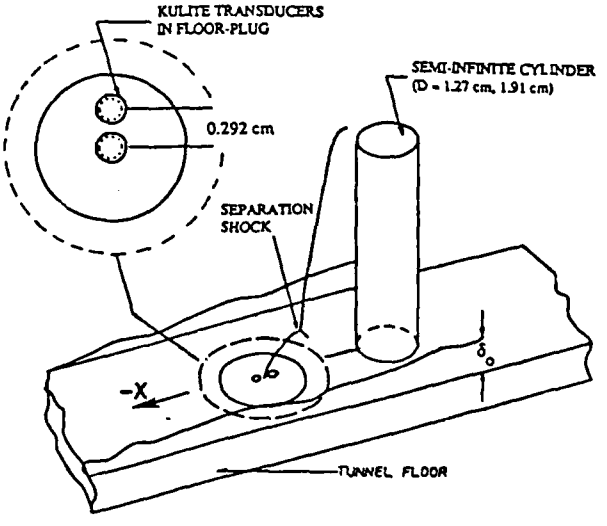

Figure 2 Model and Coordinate System

Instrumentation

A circular instrumentation plug was installed flush with the tunnel floor approximately 0.74 m from the nozzle throat. The cylinders were mounted a short distance downstream of the instrumentation plug location. Wall pressure measurements were made using miniature high frequency pressure transducers. Kulite models XCQ-062-15A or XCQ-062-50A transducers were used for all tests. These models have a full scale range of 15 psia and 50 psia with

nominal sensitivities of 13 mV/psi and 2 mV/psi respectively. Both models have a pressure sensitive diaphragm 0.071 cm (0.062 in) in diameter, with a fully active Wheatstone bridge bonded to it. The estimated frequency response of the transducers, with covers protecting the diaphragm installed, is approximately 50 kHz. Calibration of the transducers was performed statically. Earlier work [11] has shown that static calibrations are within a few percent of dynamic calibrations. In all cases, the transducers were mounted flush with the plug surface with a streamwise spacing of 0.292 cm center-to-center.

Signals from the pressure transducers were amplified with a gain of 200-500 and analog filtered at 50 kHz. 70-400 records per channel of data (1 record = 1024 data points) were then digitized by a 12 bit A/D converter (0-10 volts input) at sampling rates of 200, 250, 333, and 500 kHz per channel and stored on magnetic tape. All data acquisition and subsequent analysis was performed on a MASSCOMP MC-5500 series minicomputer.

Cross Correlation Analysis Method

The purpose of this analysis was to determine if the flow direction immediately downstream of the separation shock could be deduced from wall pressure fluctuations. Since the direction of the undisturbed boundary layer flow upstream of the shock is known, the moving shock wave is the instantaneous upstream boundary of the flowfield where flow direction near the wall is not known. Only those data corresponding to flow downstream of the shock were needed in order to analyze the flow in this region. Therefore, the first step was the development of an algorithm to isolate that fraction of the pressure signal corresponding to flow downstream of the shock. Two methods were devised and tested, both yielding similar results.

In both techniques, a two-threshold method was used. In all cases, the upstream transducer signal was used to determine when both transducers were downstream of the shock. If the upstream transducer is downstream of the shock, it follows that the downstream transducer must be also. The first threshold, PT1, was "eyeballed" at an estimated pressure value that would represent typical pressure levels downstream of a shock. PT1 was also large enough to exclude the initial pressure rise (rising edge) due to the shock passage (Figure 3). The second threshold, PT2, was set at a pressure value too low to be considered a value downstream of the shock. PT2 was also eyeballed and is also shown in Figure 3.

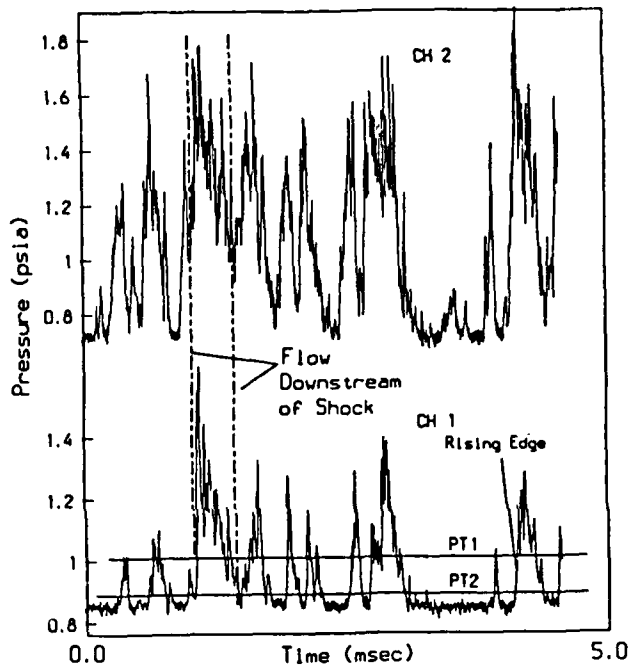

Figure 3 Pressure Time Histories and Conditional Algorithm Thresholds

Each shock passage is different so the thresholds, particularly PT1, for a given run can sometimes result in valid data being discarded. Or it may start the extracted data set too soon and include data with shock passage fluctuations. However, the results are not particularly sensitive to physically reasonable threshold settings. A brief discussion of threshold sensitivity is presented in the appendix.

In summary, the first algorithm used just the two thresholds alone to find data downstream of the shock. The second method added one further constraint. Once the level of the signal exceeded the first threshold, each data point was examined to find the maximum on the rising edge of the signal. This is referred to as the "top-finding " algorithm. Once past the maximum, the data were assumed to be associated with flow downstream of the shock until values dropped below PT2, indicating the passage of the shock downstream. This approach removes some of the inflexibility of having two "hard-set" threshold values.

The technique for finding flow direction relies on the cross correlation of two fluctuating pressure signals from two streamwise transducers located relatively close to each other. The cross correlation equation is shown below:

$$R_{pp}(\tau) = \Sigma\, p_1(t)^* p_2(t+\tau)$$

where: $p_1(t)$ is the upstream channel of pressure data
$p_2(t)$ is the downstream channel of pressure data
τ is the time delay between channels.

In general, for continuously sampled data, cross correlations are not calculated as shown, but are computed using Fast Fourier Transform (FFT) algorithms. FFT methods were developed to reduce the computation time needed for the analysis of large data sets. Typically 512 or 1024 point transforms are calculated and the correlation coefficients are averaged over many records. The time savings in using a FFT algorithm on a small data sample is not nearly as great. Also, the algebraic calculation is much simpler to code especially when the calculation data set size needs to be flexible, as was the case here, as described below. Thus the cross correlations in this analysis were calculated algebraically.

The mechanics of the calculation of cross correlations downstream of the shock proceeded as follows. The number of data points (NI) desired for each "conditionally extracted analysis data set" (CEADS), typically 32, 64, or 128 points is input to the code. The number of points chosen depends on the intermittency of the data. Data at higher intermittencies have longer continuous blocks of data behind the shock, thus allowing longer CEADS. Lower intermittency values require shorter CEADS. A counter was set at the beginning of the data file on the upstream channel and marched through the datafile. When the first threshold (PT1) criterion was satisfied, a second counter was started. NI data points past the first counter's position were examined to see that all data points satisfied the second threshold (PT2). If a data point violated the second threshold (i.e. P(t) is less than PT2), the first counter was set to the second counter's position, and searching began again. If no data points violating PT2 were encountered and the second counter reached the user-set value, the data between the two counters formed a new CEADS. This data set was algebraically cross correlated with the corresponding data points from the downstream transducer. Once the cross correlation calculations were complete, the coefficients were normalized by the product of the RMS's of the CEADS for each channel in the data set and added to a cumulative results array. The data set counter was advanced by one, the first counter was moved to the end of the current CEADS, and the searching process was started over. When all data were analyzed, the results array was normalized by the number of CEADS analyzed.

Discussion of Results

For reference purposes when discussing the cross correlations from the conditional analysis algorithm in the intermittent region, Figure 4 shows a standard 1024 point FFT cross correlation result from 400 records of data taken with two pressure transducers located in the undisturbed turbulent boundary layer. The single maximum at positive τ_o is generated by turbulent eddies traveling downstream. From τ_o and the transducer spacing the broad band convection velocity of the pressure carrying eddies can be calculated. Its value of 0.67 U_∞ (496 m/s), obtained by interpolation of the data points bracketing the maximum, agrees with previous work [12]. In contrast, downstream of 'S,' the separation line from the surface tracer experiments, two maxima in R_{pp} are evident and correspond to two physical phenomena (Fig. 5). The $R_{pp_{max}}$ at positive time delay corresponds to pressure fluctuations due to eddies in the separated shear layer flowing downstream. The broadband time delay for maximum correlation of these structures is τ=0.006-0.008 msec, giving a downstream convection velocity in the range 365-487 m/sec. This velocity is less than that in the undisturbed boundary layer since the flow has gone through the shock wave. The second phenomenon is backflow in the recirculating/vortical separated structure. This backflow generates the peak at τ=-0.016 to -0.018 msec, corresponding to a broadband upstream velocity of 162-183 m/sec.

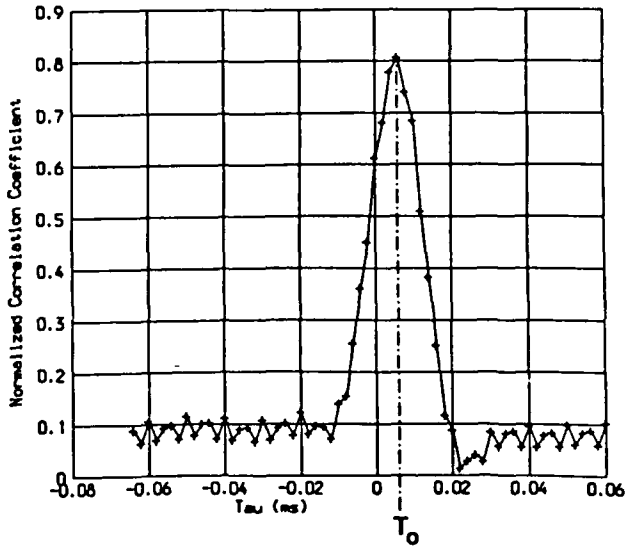

Figure 4 Standard Cross Correlation of Undisturbed Turbulent Boundary Layer

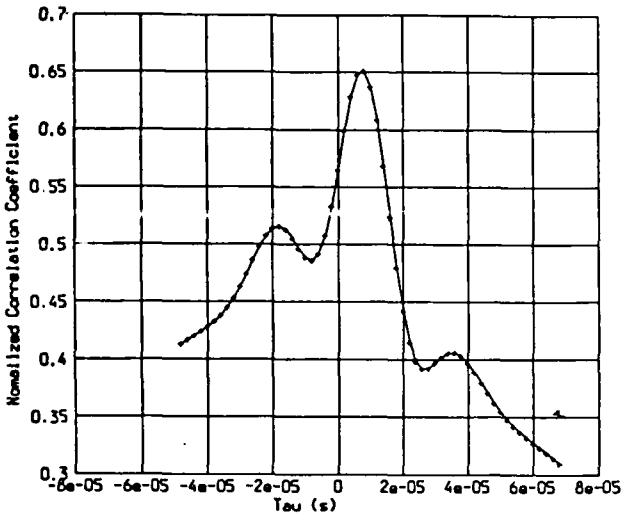

Figure 5 Standard Cross Correlation of Flow Downstream of 'S'

As discussed earlier, the conditional analysis space time correlation code was written to analyze signals in the intermittent region. Figure 6 shows correlations at five stations in the intermittent region for the 1.9 cm diameter cylinder. The legend indicates the normalized streamwise station of each transducer, the intermittency of the upstream channel and the number of CEADS used to calculate each curve. At all values of intermittency, the "double peak" characteristic of separated flow can be seen. The positive and negative values of τ at which these maxima in R_{pp} occur are the same in all five cases. Based on the transducer spacing and τ, the broadband upstream and downstream velocities are in the ranges of 195-292 and 292-584 m/sec respectively. The boundaries of these ranges are calculated using the data points bracketing the peaks. From linear interpolation the actual maxima appear to be about mid-way between these points, giving upstream and downstream velocities of 234 and 390 m/sec respectively. Further, taking into account the lower sampling rates for the data sets in the intermittent region and the reduced time resolution of the cross-correlations, these velocities are the same as those indicated by Figure 5. These results show clearly the flow structure downstream of the instantaneous shock location is the same at all stations within the intermittent region. Further, it is the same as the flow structure in the separated flow downstream of 'S.'

Figure 7 shows cross correlations using the 1.27 cm diameter cylinder. All three stations show the characteristic "double peak", indicating backflow immediately behind the shock. No variation in time delay at $R_{pp_{max}}$ is seen. $R_{pp_{max}}$ occurs at τ=-0.014 msec and τ=0.08-0.01 msec giving upstream and downstream velocities of 209 and 292-365 m/sec respectively. Examination of Figures 6 and 7 reveals that both cylinders have the same time delays for both peaks, within the sampling rate accuracy, indicative of the same flow structure immediately downstream of the shock.

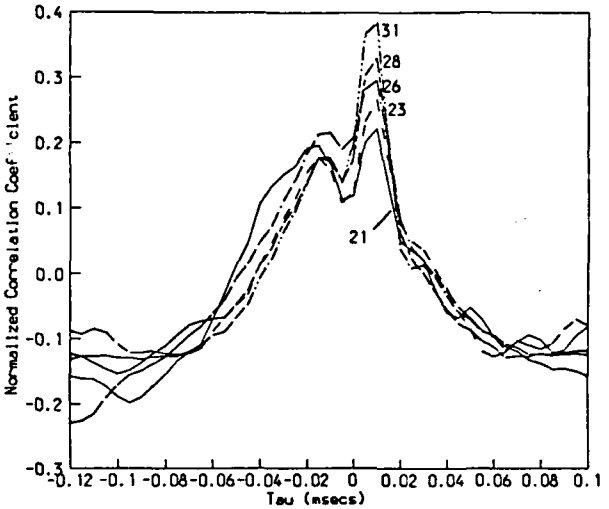

Run	X/D1	X/D2	Gamma1	No. of CEADS
21	2.89	2.73	8.47	133
23	2.83	2.68	15.9	222
26	2.63	2.47	32.4	1457
28	2.57	2.42	37.73	1229
31	2.37	2.21	75.5	3018

Figure 6 Cross Correlations of CEADS-1.9 cm Cyl.

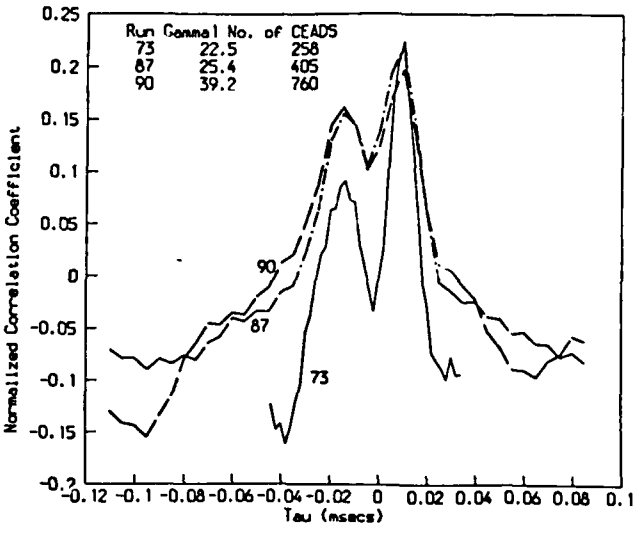

Figure 7 Cross Correlations of CEADS-1.27 cm Cyl.

Conclusions

A method of detecting flow direction downstream of the unsteady separation shock using fluctuating wall pressure signals has been developed and tested in a Mach 5 shock wave turbulent boundary layer interaction induced by circular cylinders. In this method, flow direction is deduced from cross correlations of that part of the pressure signal downstream of the moving shock wave. The results show:

(1) For all cylinder flows examined the cross correlations show a maximum R_{pp} at negative time delay indicating that backflow exists immediately downstream of the shock at all stations in the intermittent region.

(2) Separation essentially occurs across the shock in the intermittent region upstream of unswept circular cylinders and hence the separation point itself undergoes a large scale streamwise motion. It appears that the well defined separation line from the kerosene lampblack pattern delineates the downstream boundary of a region of intermittent separation.

Acknowledgements

This work was sponsored in part by AFOSR Grant 86-0112 (monitored by Dr. James Wilson and Dr. James McMichael), ARO Grant DAALO3-6-0045, (monitored by Dr. Robert Singleton), and the Center of Excellence of Hypersonics Training and Research at the University of Texas at Austin (supported by NASA, AFOSR, and ONR). These sources of support are gratefully acknowledged.

References

[1] Settles, G. S., "An Experimental Study of Compressible Turbulent Boundary Layer Separation at High Reynolds Numbers," PhD. Dissertation, Mech. and Aero. Engineering Department, Princeton University, Sept. 1975.

[2] Dolling, D. S., and M. T. Murphy, "Unsteadiness of the Separation Shock Wave Structure in a Supersonic Compression Ramp Flowfield," *AIAA Journal*, Volume 21, December 1983, pp. 1628-1634.

[3] Dolling, D. S., and C. T. Or, "Unsteadiness of the Shock Wave Structure in Attached and Separated Compression Ramp Flowfields," *Experiments in Fluids*, Vol. 3, 1985, pp.24-32.

[4] Muck, K. C., J. P. Dussauge, and S. M. Bogdonoff, "Structure of the Wall Pressure Fluctuations in a Shock-Induced Separated Turbulent FLow,", AIAA Paper 85-0179, Jan. 1985.

[5] Dolling, D. S. and J. C. Narlo II, "Driving Mechanism of Unsteady separation Shock Motion in Hypersonic Interactive Flow," AGARD Conference on "Aerodynamics of Hypersonic Lifting Vehicles," AGARD Cp-428, April 1987.

[6] Dolling, D. S. and Brusniak L., "Separation Shock Motion in Fin, Cylinder, and Compression Ramp-Induced Turbulent Interactions," AIAA Paper 87-1368, June 1987.

[7] Smith, D. R., and D. S. Dolling, "Unsteady Shock-Induced Turbulent Separation in Mach 5 Cylinder Interactions," AIAA Paper 88-0305, Jan 1988.

[8] Eaton, J. K., A. H. Jeans, J. Ashjaee, and J. P. Johnston, " A Wall-Flow Direction Probe for use in Separating and Reattaching Flows," *Journal of Fluids Engineering*, Vol. 101, September 1979, pp. 364-366.

[9] Westphal, R. V., J. K. Eaton, and J. P. Johnston, "A new Probe for Measurement of Velocity and Wall Shear Stress in Unsteady, Reversing Flow," *Journal of Fluids Engineering*, Vol. 103, September 1981, pp.478-482.

[10] Dolling, D. S., and S. M. Bogdonoff, "Scaling of Interactions of Cylinders with Supersonic Turbulent Boundary Layers," *AIAA Journal*, Vol. 19, No. 5, May 1981, p. 655-657.

[11] Raman, K. R., "A Study of Surface Pressure Fluctuations in Hypersonic Turbulent Boundary Layers," NASA CR-2386, Feb 1974.

[12] Tran, T. T., "An Experimental Investigation of Unsteadiness in Swept Shock Wave/Turbulent Boundary Layer Interactions," Ph.D. Dissertation, Mech. and Aero. Engineering Department, Princeton University, Oct 1986.

Appendix

Conditional sampling/analysis algorithms are a relatively new type of analysis being used in these types of interactive flows. When data is converted into a new signal, box cars (0's or 1's) for shock motion analysis for instance, or split into different segments based on given criteria, the sensitivity of the method to the decision criteria should be investigated. This was recently discussed by Dolling and Brusniak[6] regarding box car analysis. To confirm the validity of the conditional analysis space-time correlation code, a threshold sensitivity analysis was performed.

Figure 8 shows the conditional analysis cross-correlation results for different thresholds for the same set of data. Two cases are shown for clarity. Although the magnitudes of the coefficients have changed, the positive and negative values of $R_{pp_{max}}$ remain at the same time delays (τ). This was also observed for several other threshold

combinations. Thus, although the values of $R_{pp_{max}}$ fluctuate, the corresponding values of τ are insensitive to changes in threshold values.

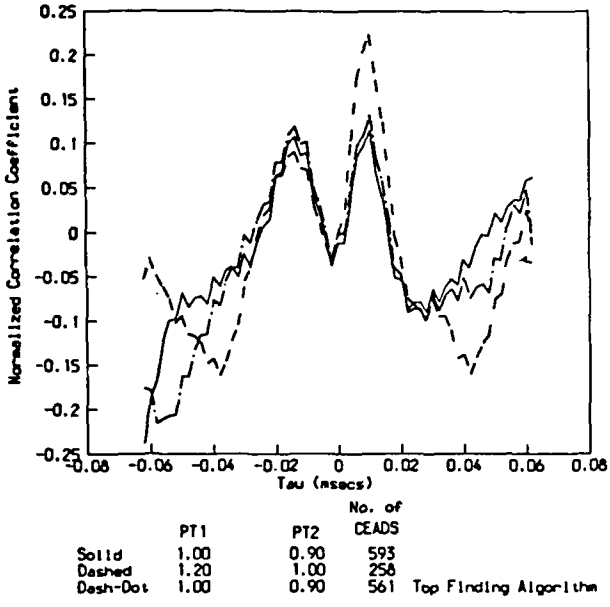

Figure 8 Sensitivity of Cross Correlations of CEADS

A similar result is obtained when comparing algorithms. Figure 8 shows results for both algorithms tested. Each case had the same thresholds. The top finding algorithm had fewer CEADS which met the 32 point analysis data set requirement due to the stricter requirement of starting the data set with the maximum point past the first threshold, PT1. As a result, more fluctuations due to the shock passage were eliminated, and the corresponding correlation values due to flow behind the shock are slightly higher. However, the time delay values for the peaks remain unaffected.

Appendix B

Flowfield Model

The reason why the surface streak lines are in the downstream direction upstream of 'S' can be explained using a relatively simple model. Consider the flow on centerline. If the instantaneous surface shear stress in the intermittent region is modelled as a step function (Fig.13), then the mean wall shear, $\bar{\tau}_w$, which the surface streaks respond to, is given by

$$\bar{\tau}_w = (1-\gamma)\,\bar{\tau}_u + \gamma\,\bar{\tau}_d$$

where $\bar{\tau}_u$ and $\bar{\tau}_d$ are the average wall shear stresses in the upstream and downstream zones. $\bar{\tau}_w$ will equal zero when

$$\frac{\gamma - 1}{\gamma} = \frac{\bar{\tau}_d}{\bar{\tau}_u}.$$

Since $\bar{\tau}_u$ is the wall shear stress of the incoming supersonic boundary layer and $\bar{\tau}_d$ is at the upstream boundary of the separated flow, the ratio $\bar{\tau}_u/\bar{\tau}_d$, given by N will be large. Hence, $\bar{\tau}_w = 0$ when $\gamma = N/(1+N)$. For large values of N, γ is close to 1. Thus the mean shear stress at the wall can be in the downstream direction even when the flow is separated for the major fraction of the time.

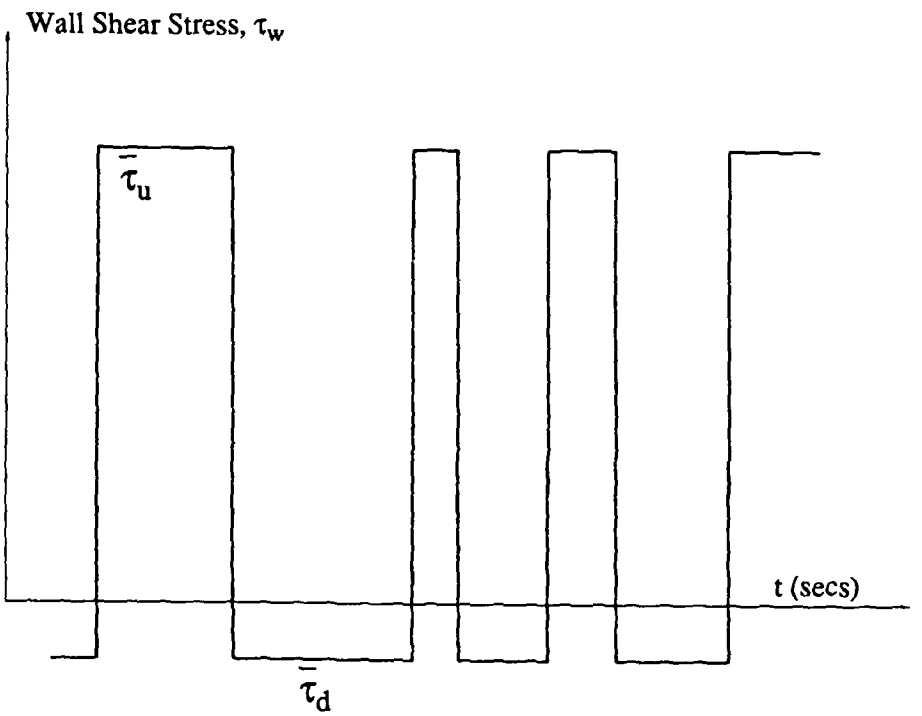

Figure 13 - Shear Stress Model